Molecular jet study of van der Waals complexes of flexible molecules: n-Propyl benzene solvated by small alkanes[a)]

K. S. Law and E. R. Bernstein

Citation: The Journal of Chemical Physics **82**, 2856 (1985); doi: 10.1063/1.448287
View online: http://dx.doi.org/10.1063/1.448287
View Table of Contents: http://aip.scitation.org/toc/jcp/82/7
Published by the American Institute of Physics

Molecular jet study of van der Waals complexes of flexible molecules: *n*-Propyl benzene solvated by small alkanes[a)]

K. S. Law and E. R. Bernstein
Department of Chemistry, Condensed Matter Sciences Laboratory, Colorado State University, Fort Collins, Colorado 80523

(Received 27 August 1984; accepted 28 November 1984)

A combination of atom–atom potential calculations and experimental molecular jet spectroscopic studies is used to elucidate the geometry and binding energy of *n*-propyl benzene/methane, ethane, and propane clusters. Two color time-of-flight mass spectroscopy data and calculations are presented for both *trans* and *gauche* configurations of *n*-propyl benzene with up to three hydrocarbon molecules of solvation. Cluster shifts and geometry are treated in detail for the observed and calculated systems. Solvation, as observed in the clusters, seems to have little effect on the geometry of the solute in this instance. Alkyl chain motion is also discussed for the *n*-propyl benzene isolated molecule.

I. INTRODUCTION

Supersonic molecular jet spectroscopy of van der Waals (vdW) clusters is capable of generating information which can lead to a fundamental understanding of intermolecular interactions. The vdW cluster shift, binding energy, and energy dissipation dynamics are experimental observations essential for the characterization of the solvation state and processes.[1] The cluster shift has become of particular interest: besides being dependent on the polarizability of the solvent and solute molecules, the cluster shift is a sensitive function of the cluster geometry[1(a),2] and thereby the local site details of the intermolecular potential.

In addition, the study of vdW complexes consisting of a flexible solute molecule solvated by small hydrocarbons is of interest for at least two reasons. First, information is obtained on the effect of solvation on solute geometry. Second, if the solute molecule assumes a few special geometries, the effect of these different geometries on the solvation processes themselves can be measured. The present study of *n*-propyl benzene (npb) sheds light mainly on this latter issue.

Solvation studies of npb should provide a unique opportunity to pursue the above relationships further as npb exhibits two distinct conformations in a supersonic expansion—*trans* and *gauche*.[3] (We adopt the nomenclature of Ref. 3 for convenience and to avoid confusion; however, we feel *trans* and *cis* are probably more appropriate and consistent terms for npb.) In the *trans* conformation (ntpb), the propyl chain extends away from the aromatic ring, whereas in the *gauche* conformation (ngpb), the propyl chain folds back over the ring and partially covers one side of it (see Fig. 1). Thus, both the top and bottom of the ring are exposed in ntpb and are expected to provide lowest energy binding sites for solvent molecules.[2] Only one side of the ring ("the bottom") is completely exposed for binding solvent in the *gauche* conformation. Solvation of ntpb and ngpb by small hydrocarbons should yield different cluster shifts as the cluster geometries are expected to be modified by the two different conformations of the propyl chain.

Some preliminary information on the solvation of npb by helium is already available.[3(a)] Two features, assigned to ntpb$(He)_{1,2}$, are reported on the high energy side of the ntpb first singlet 0_0^0 transition: the features are identified as belonging to the ntpb ring centered He complexes. Under the same experimental conditions only one blue shifted feature is formed for the 0_0^0 transition of ngpb. This latter observation is attributed to the partial blocking of a potential ring binding site by the propyl side chain and thus only one He–ngpb complex is readily formed.

The present work examines the solvation of npb by methane, ethane, and propane molecules. We report on three specific investigations in the paper: (1) 0_0^0 absorption spectra observed through two-color photoionization time of flight mass spectroscopy (two-color MS); (2) two-color MS studies of higher vibrational levels of the excited state to determine binding energies; and (3) atom–atom potential calculations (exp-6) to predict the minimum energy configurations of different clusters.

Through these studies it is found that the binding energies of npb–alkane clusters are similar to those of the comparable toluene–alkane clusters.[2(a)] The presence of the propyl chain, however, in npb generates additional interactions which significantly modify the overall cluster geometry. The binding sites for an alkane solvent molecule above (A, on the same side as the propyl chain) or below (B, on the side opposite from the propyl chain) the aromatic ring are not equivalent. The data obtained in these studies suggest that rotation of the propyl chain does not occur about the phenyl–alkyl bond (C_1–C_7) or the C_7–C_8 bond.

II. EXPERIMENTAL PROCEDURES

The procedures for obtaining two-color MS absorption spectra and the apparatus employed for this study

[a)] Supported in part by grants from ONR and ARO-D.

 0021-9606/85/072856-11$02.10

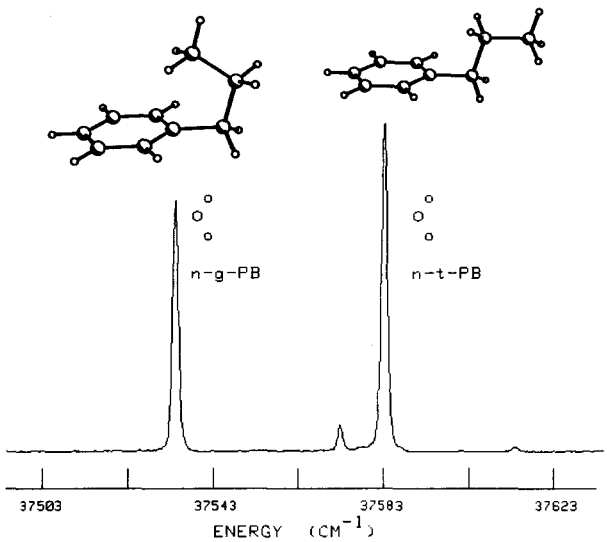

FIG. 1. Two-color MS spectrum of npb at the 0_0^0. The electronic origins for ngpb and ntpb are observed at 37 533.9 cm^{-1} and 37 583.1, respectively. Experimental conditions: 0.5 mm pulsed nozzle operated at 10 Hz; nozzle temperature = 25 °C, backing pressure P_0 = 100 psi, ionization wavelength = 3050 A.

have been described in detail previously.[1a] Commercial grade npb is used in this work without purification. Two Quanta Ray Nd:YAG lasers are used to pump two dye laser-doubling systems which provide the pump and ionization beams. The excitation to S_1 of npb is accomplished with doubled Coumarin 500 dye output. S_1 to npb$^+$ ionization is affected by doubled R640 output (I.P. = 8.72 eV).[4] The expensive, short lived Coumarin 500 dye is recovered by recrystallization techniques.[5]

Calibration of the absorption spectra is provided by the optogalvanic effect for a Fe:Ne hollow cathode lamp. The absolute positions of spectral features are accurate to ± 1.0 cm^{-1}.

Atom–atom potential calculations employ the simple exp-6 form,

$$E_{ij} = -\frac{A_{ij}}{R_{ij}^6} + B_{ij}\exp[-C_{ij}R_{ij}].$$

The aromatic coefficients A, B, and C of benzene are used for npb.[6] The aliphatic coefficients of ethane and propane are assumed to be the same as those of methane.[7] The aliphatic–aromatic (al–ar) coefficients are derived as follows:

$$A_{\text{al-ar}} = (A_{\text{al-al}}A_{\text{ar-ar}})^{1/2},$$

$$B_{\text{al-ar}} = (B_{\text{al-al}}B_{\text{ar-ar}})^{1/2},$$

$$C_{\text{al-ar}} = \tfrac{1}{2}(C_{\text{al-al}} + C_{\text{ar-ar}}).$$

The complete set of coefficients employed in this study is given in Table I.

The calculation is carried out with an HP 9845 S computer. The aromatic ring of the npb solute molecule is held fixed in the XY plane with the coordinate system origin at the ring center. The propyl chain is assumed to be fixed (see Fig. 1) and in the $+Z$ direction above (A) the plane of the ring in either the g or t configuration. The carbon atoms of the propyl chain are in the molecular symmetry plane perpendicular to the plane of the ring.

The alkane solvent molecule is introduced systematically in a random orientation relative to npb and the sum of the nonbonded atom pair energies is minimized with respect to the six degrees of rotational and translational freedom of the solvent molecule. The total energy of the cluster is minimized with an increment or decrement of 0.01 Å for translational and 1° for rotational motion until a local energy minimum is found. This general process is then repeated by introducing the alkane solvent molecule in another orientation relative to npb until all reasonable local minima are located. For clusters involving two alkane solvent molecules, only one solvent molecule is allowed to move at a time: many iterations are required to achieve a local energy minimum in this instance. In general, two or three local minima are found for a specific npb–alkane cluster. Only the minimum energy configuration, or configurations nearly isoenergetic with it, are chosen as optimum cluster conformations.

III. RESULTS

Detailed two-color MS study of npb–$(C_yH_{2y+2})_x$ ($y \leq 3$, $x \leq 3$) clusters is limited to the 0_0^0 transitions as this region is relatively free of spectral congestion. Higher vibronic transitions are probed only to bracket the cluster binding energies. Fluorescence excitation and dispersed emission studies are omitted from this report because: (a) the fluorescence excitation experiment is not mass selective and it thus produces only redundant information; (b) preliminary two-color MS studies indicate $(npb)_2$ has a strong absorption in the spectral region of interest[8]; and (c) dispersed emission studies of the toluene–alkane systems show extensive intramolecular vibrational redistribution[2] and npb–alkane clusters are expected to behave similarly.

In this section we present experimental and calculational data on the cluster 0_0^0 spectra and binding energies. We begin, however, with a short description of the npb spectra.

TABLE I. Atom–atom potential parameters (see Ref. 6).

	A (cm^{-1} A^6/mol)	B (cm^{-1}/mol)	C (Å)
Aliphatic–aliphatic			
C–C	131 096.216	8 890 353.173	3.421
C–H	47 829.961	7 562 708.563	3.940
H–H	15 028.103	6 390 527.943	4.643
Aliphatic–aromatic			
C–C	162 645.059	16 520 286.388	3.511
C–H	47 863.504	6 434 084.510	3.805
H–H	13 070.695	2 497 532.635	4.192
Aromatic–aromatic			
C–C	201 786.260	30 696 427.500	3.600
C–H	47 897.070	5 473 891.150	3.670
H–H	11 368.240	976 080.430	3.740

A. npb spectra

In order to understand the two-color MS spectra of npb–alkane clusters, a description of the absorption spectrum of the npb molecule itself is necessary. A portion of the npb two-color MS spectrum near the electronic origin is presented in Fig. 1. The two nearly equal intensity bands at 37 533.9 and 37 583.1 cm^{-1} correspond to the electronic origins of ngpb and ntpb, respectively. The 0_0^0 of ngpb is red shifted 49.2 cm^{-1} relative to the 0_0^0 of ntpb due to a "self-solvation" of the aromatic ring by the propyl group.[3a] The two weak features at 37 572.9 and 37 613.9 cm^{-1} are probably related to the hindered rotations of parts of the propyl chain (in particular, the terminal methyl group).

B. Origin cluster spectra

The assignment of the cluster spectra largely relies on the potential calculations and the experience obtained from toluene–alkane and benzene–alkane systems reported previously from our laboratory.[2] The present calculations suggest that the preferred binding sites in npb are above (A, $+Z$) and below (B, $-Z$) the aromatic ring. (Recall that the t or g propyl chain is assumed to be above the ring.) A general consistent picture emerges through consideration of the observed two-color MS spectra and the calculated minimum energy cluster configuration. The cluster red shift appears to be strongly dependent on the effective interaction ("distance") between the solvent molecule and the π cloud of the aromatic ring of npb: the larger interaction is associated with the larger cluster red shift. Similar results are reported for toluene–alkane and benzene–alkane systems.

For a ring centered toluene or benzene–alkane cluster, the cluster red shift of the $S_1 \leftarrow S_0$ transition is $\sim 55 \pm 15$ cm^{-1}; the exact number depends upon the solvent molecule involved. The npb cluster shifts are expected to be somewhat larger than this because npb probably has a larger polarizability than toluene or benzene.

In the following assignment and analysis of the spectra of the various npb–solvent clusters, the transitions for each cluster are typically presented in order of increasing energy. We have done this to allow the reader to follow the logic of the assignments free from the prejudice of an overriding theme. The general trends and systematics of the results will be outlined in Sec. IV.

1. $npb(CH_4)_x$

Figure 2 (bottom trace) depicts the two-color MS spectrum of the $npb(CH_4)_1$ origin. The band at -93.4 cm^{-1} relative to the ntpb 0_0^0 (-44.2 cm^{-1} relative to the 0_0^0 of ngpb) is assigned as the 0_0^0 of the B configuration of $ngpb(CH_4)_1$ (see Fig. 3). Potential calculations indicate both the A (above the ring, with the chain) and B (below the ring, away from the chain) configurations of $ngpb(CH_4)_1$ are possible with similar binding energies. However, in the A configuration the methane molecule has a considerable displacement from the ring center and a concomitant large interaction with the terminal methyl group of the propyl chain of ngpb. The A configuration of ngpb is therefore not likely to have a cluster shift as large as -40 cm^{-1}: we have, in fact, been unable to identify the A $ngpb(CH_4)_1$ configuration in the $npb(CH_4)_1$ spectra.

The intense peak at -51 cm^{-1} relative to the ntpb 0_0^0 can be assigned as the 0_0^0 of the A configuration of $ntpb(CH_4)_1$. This feature is followed by progressions in vdW stretching and bending modes: tentative assignments are tabulated in Table II. In the ntpb A configuration the methane molecule centers above the aromatic ring as shown in Fig. 3 and thus generates a considerable cluster spectral shift. Repeated measurements of the doublet structure at -26 cm^{-1} indicate that this doublet structure is not an experimental artifact. One of these components

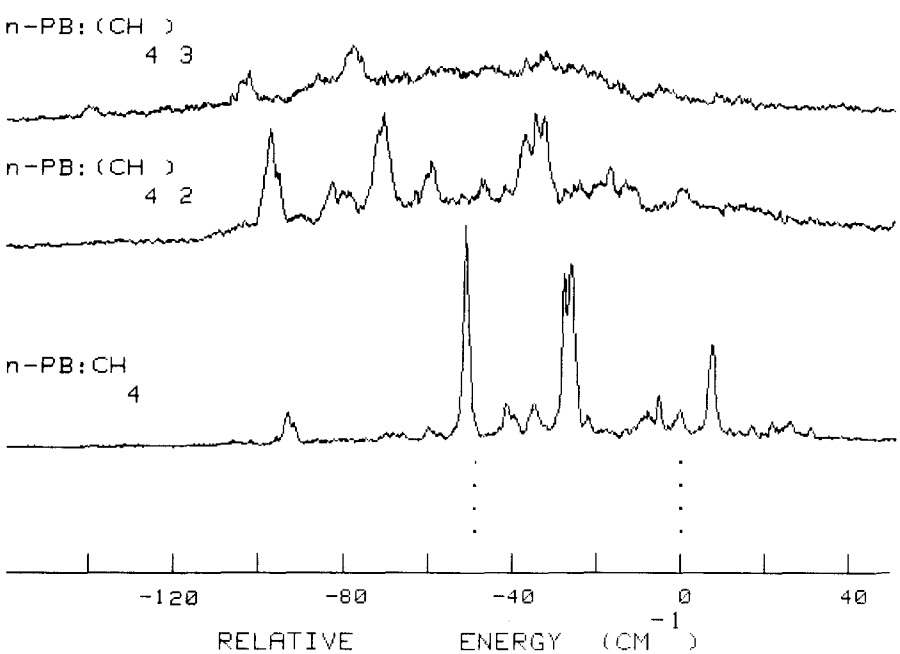

FIG. 2. Two-color MS spectra of $npb(CH_4)_x$, $x \leq 3$ observed at the 0_0^0 with 2% CH_4 in the expansion with helium carrier gas. Intensity scale is different for each cluster. The energy scale is relative to the ntpb 0_0^0 at 37 583.1 cm^{-1}. Dotted lines indicate the 0_0^0 of ngpb (lower energy) and ntpb. Experimental conditions: see Fig. 1.

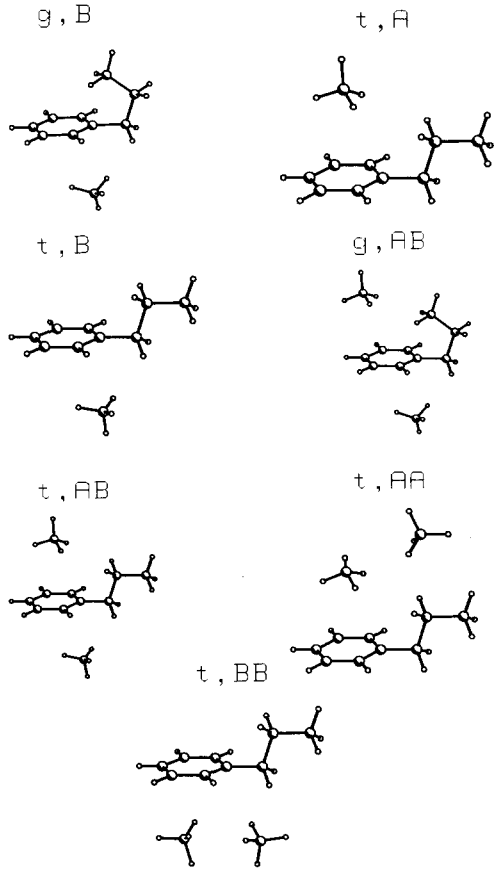

FIG. 3. Minimum energy configurations of $npb(CH_4)_x$, $x \leq 2$ as obtained from potential calculation. The order of the cluster configurations is arranged according to Table II. *t*, B: indicates the solvent alkane molecule binds below the aromatic ring of ntpb. *g*, AB: indicates the solvent alkane molecules bind above and below the aromatic ring of ngpb. "Above the ring" refers to the side of the ring (+*Z* direction) with the propyl chain and "below the ring" (−*Z* direction) refers to the side of the ring without the propyl. The propyl chain extends in the +*X* direction. The atomic coordinates of the methane molecule in *g*, A are identical to those of the methane molecule binding above the aromatic ring in *g*, AB. Detailed atomic coordinates of the clusters can be provided upon request.

is reasonably assigned as a stretch built on the A $ntpb(CH_4)_1$ origin; the other feature, however, must derive from another configuration of $ntpb(CH_4)_1$. Potential calculations suggest that the only other configuration of $ntpb(CH_4)_1$ which has a significant binding energy is the B configuration (see Fig. 3).

The calculations indicate that the CH_4 molecule in the B configuration is shifted towards the propyl chain and away from the ring center. Based on these assignments, the propyl chain has a significant influence on the overall cluster geometry and spectral shifts.

The tentative assignments of the two-color MS spectrum of $npb(CH_4)_2$ (see Fig. 2, middle trace) are given in Table II. The assignments are made with the support of the potential calculations and in conjunction with the above observations. Coordination of a CH_4 solvent molecule above the aromatic ring (at the A site) of the B configuration of $ngpb(CH_4)_1$ would probably have only a small effect on the B $ngpb(CH_4)_1$ cluster shift because, as can be seen in Fig. 3, this second "A methane" has a relatively small direct interaction with the aromatic ring. Thus the band at -96.4 cm^{-1} (-47.2 cm^{-1} relative to the 0_0^0 of ngpb) may well be the AB configuration of $ngpb(CH_4)_2$, as the BB configuration would have an increased shift [see $ngpb(C_2H_6)_1$ assignment below]. The intense feature at -70 cm^{-1} can be reasonably assigned as the 0_0^0 of the AB configuration of $ntpb(CH_4)_2$ based on the nearly additive (51 + 26 cm^{-1}) spectral shifts for this peak. Potential calculations also identify both the AA and BB $ntpb(CH_4)_2$ configurations as stable with good binding energies; the AA configuration should have the larger of the two spectral shifts (see Fig. 3). The bands at -58.6 and -36.2 cm^{-1} are thereby assigned as the 0_0^0 transitions of the AA and BB configurations of $ntpb(CH_4)_2$, respectively.

Figure 2 (top trace) presents the two-color MS spectrum of $npb(CH_4)_3$. Two main features are apparent above a broad background. The bands at -103.2 cm^{-1} (-54 cm^{-1} relative to the 0_0^0 of ngpb) and -77.6 cm^{-1} appear to correspond to the 0_0^0 transitions of the ABB configurations of $ngpb(CH_4)_3$ and $ntpb(CH_4)_3$, respectively. Again, additivity of cluster spectral shift is the main factor in the assignment. The weak feature at -139.7 cm^{-1} remains at present unassigned.

2. $npb(C_2H_6)_x$

The two-color MS detected spectrum of $npb(C_2H_6)_1$ evidences a rich array of spectral features (see Fig. 4, bottom trace). Calculations indicate that the ethane atomic coordinates of the B configurations of $ngpb(C_2H_6)_1$ and $ntpb(C_2H_6)_1$ are quite similar; a detailed examination of the coordinates, however, reveals that the π-cloud solvent interaction is a little stronger for the $ngpb(C_2H_6)_1$ B configuration. Hence, we assign the bands at -80.6 cm^{-1} (-31.4 cm^{-1} relative to the 0_0^0 band of ngpb) and -26.3 cm^{-1} as the 0_0^0 transitions of the B configurations of $ngpb(C_2H_6)_1$ and $ntpb(C_2H_6)_1$, respectively. The intense peak at -62.8 cm^{-1} probably corresponds to the 0_0^0 of the A configuration of $ntpb(C_2H_6)_1$ since the ethane solvent apparently has the largest effective interaction with the aromatic ring in this geometry (see Fig. 5). The remaining features in the spectrum can be assigned as vdW vibrations of the $npb(C_2H_6)_1$ clusters built on these three origins (ntpb A, ntpb B, and ngpb B). Detailed but tentative assignments of these spectra are presented in Table III. We are unable to identify an A $ngpb(C_2H_6)_1$ species in the observed spectrum of $npb(C_2H_6)_1$.

The two-color MS spectrum of $npb(C_2H_6)_2$ is quite complicated (Fig. 4, middle trace): suggested assignments are presented in Table III. The assignments are made in accordance with the observed data for $npb(C_2H_6)_1$ and the potential calculations for $npb(C_2H_6)_2$. The -85.2 cm^{-1} feature is assigned as the 0_0^0 of the AB configuration of $ntpb(C_2H_6)_2$ based on the additive (26.3 + 62.8 cm^{-1}) spectral shift. The -96.8 cm^{-1} (-47.6 cm^{-1} relative to the 0_0^0 of ngpb) and -48.7 cm^{-1} bands are most probably the 0_0^0 transitions of the BB configurations of the $ngpb(C_2H_6)_2$ and $ntpb(C_2H_6)_2$ clusters. The latter identifications derive from the calculations and $npb(C_2H_6)_1$

TABLE II. Two-color MS absorption features of npb$(CH_4)_x$, $x \leq 3$ near the electronic origin.[a]

Energy (vac. cm^{-1})	Energy relative to cluster 0_0^0 (cm^{-1})	Energy relative to ntpb 0_0^0 (cm^{-1})	Tentative assignment[b]
npb:$(CH_4)_1$			
37 489.7	0	−93.4	ngpb(CH_4) 0_0^0 B (-44.2 cm^{-1} relative to ngpb 0_0^0)
37 523.2	33.5	−59.9	V_0^1
37 532.1	0	−51	ntpb(CH_4) 0_0^0 A
37 541.7	9.6	−41.5	X_0^1
37 548.1	16.0	−35	Y_0^1
37 555.5	23.4	−27.6	V_0^1
37 574.5	42.4	−8.6	V_0^2
37 557	0	−26.1	ntpb(CH_4) 0_0^0 B
37 590.7	33.7	7.6	V_0^1
npb$(CH_4)_2$			
37 486.7	0	−96.4	ngpb$(CH_4)_2$ 0_0^0 AB (-47.2 cm^{-1} relative to ngpb 0_0^0)
37 501.5	14.8	−81.6	X_0^1
37 504.9	18.2	−78.3	Y_0^1
37 522.5	35.8	−60.6	V_0^1
37 513.1	0	−70	ntpb$(CH_4)_2$ 0_0^0 AB
37 549.6	36.5	−33.5	V_0^1
37 524.5	0	−58.6	ntpb$(CH_4)_2$ 0_0^0 AA
37 537.1	12.6	−46	X_0^1
37 541.9	17.4	−41.2	Y_0^1
37 551.6	27.1	−31.5	V_0^1
37 572	47.5	−11	V_0^2
37 546.9	0	−36.2	ntpb$(CH_4)_2$ 0_0^0 BB
37 559.4	12.5	−23.8	X_0^1
37 565.4	18.5	−17.7	Y_0^1
37 584.5	37.6	1.4	V_0^1
npb$(CH_4)_3$			
37 479.8	0	−103.3	ngpb$(CH_4)_3$ 0_0^0 ABB (-54.1 cm^{-1} relative to ngpb 0_0^0)
37 505.5	0	−77.6	ntpb$(CH_4)_3$ 0_0^0 ABB

[a] The cluster 0_0^0 of the lowest electronic energy is tabulated first together with its vdW modes, followed by the next lowest electronic energy cluster 0_0^0 and its vdW modes. Therefore, the tabulated features are not necessarily in order of ascending energy.

[b] X, Y denote vdW bending motions and V stands for vdW stretch. A (above, with chain) and B (below, away from chain) refer to configurations of the solvent relative to the solute propyl chain position with respect to the ring plane. See the text for explanation.

data. The most intense band at -58.4 cm^{-1} is assigned as the 0_0^0 of the AA ntpb$(C_2H_6)_2$ configuration. In this configuration the interaction between the solvent and the aromatic ring of ntpb derives essentially from only one of the ethane molecules (see Fig. 5).

The major features in the two-color MS spectrum of npb$(C_2H_6)_3$ (Fig. 4 top trace) appear in the proximity of the 0_0^0 of ntpb (-35 to $+2$ cm^{-1}). Such features provide evidence for heterogeneous nucleation[2] as the dominant solvation process under the present beam conditions. In this process, the solvent molecules form a cluster before interacting with the solute species. Solvent-solvent interactions in the final solute–solvent cluster tend to reduce the number and strength of the solvent–solute interactions, eventually leading to smaller cluster red shifts. The relative positions of the major features in this spectrum are presented in Table III.

3. *npb$(C_3H_8)_x$*

Figure 6 (bottom trace) presents the two-color MS spectrum of npb$(C_3H_8)_1$. The intense band at -52.2 cm^{-1} is assigned as the A configuration of ntpb$(C_3H_8)_1$. Note that this spectral shift is nearly identical to that observed for the A configuration of ntpb$(CH_4)_1$. Calculations suggest that the effective interaction between the propane solvent molecule and the aromatic ring derives mainly from the interaction of the propane terminal methyl group and the ring (see Fig. 7). The atomic coordinates of the B configuration of ngpb$(C_3H_8)_1$ and ntpb$(C_3H_8)_1$ are quite similar;

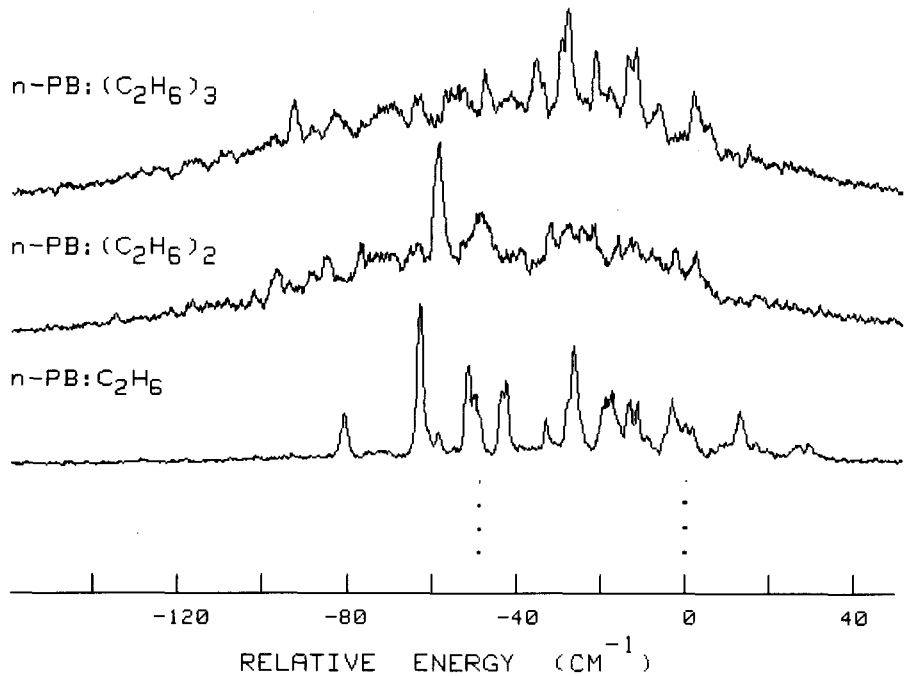

FIG. 4. Two-color MS spectra of npb$(C_2H_6)_x$, $x \leq 3$ observed at the 0_0^0 with 2% C_2H_6 in the expansion with helium carrier gas. The intensity scale is different for each cluster. Experimental conditions: see Fig. 1.

however, the B ngpb$(C_3H_8)_1$ configuration evidences a somewhat larger interaction between the propane molecule and the aromatic ring. Hence, we assign the bands at -74.1 cm^{-1} (-24.9 cm^{-1} relative to the 0_0^0 of ngpb) and -16.9 cm^{-1} as the 0_0^0 transitions of the B configurations of ngpb$(C_3H_8)_1$ and ntpb$(C_3H_8)_1$, respectively. The tentative assignments of most of the observed npb$(C_3H_8)_1$ spectral features can be found in Table IV.

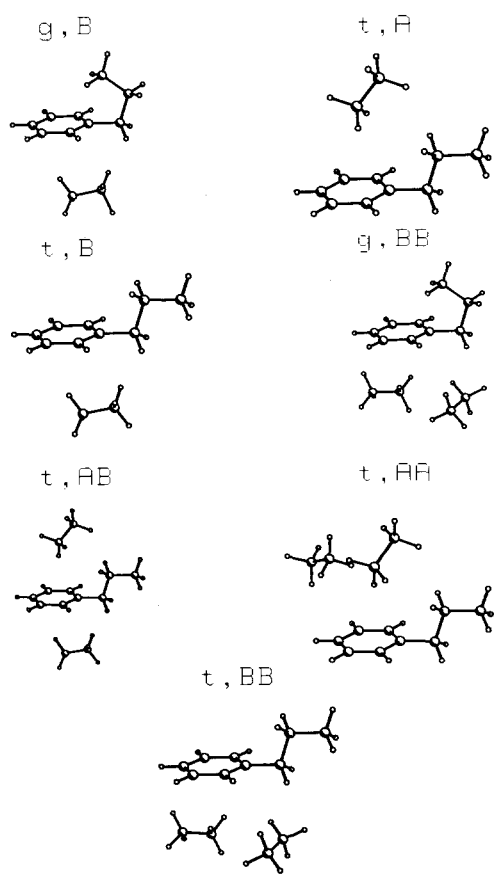

FIG. 5. Minimum energy configurations of npb$(C_2H_6)_x$, $x \leq 2$ obtained from potential calculations. The order of the configurations is arranged according to Table III. Detailed atomic coordinates of the clusters can be provided upon request.

The most intense feature in the two-color MS spectrum of npb$(C_3H_8)_2$ appears at -68.5 cm^{-1} relative to the ntpb origin (Fig. 6, middle trace); this transition can be assigned as the 0_0^0 of the AB configuration of ntpb$(C_3H_8)_2$ based on its additive (16.9 + 52.2 cm^{-1}) spectral red shift. The next most intense peak (at -75.8 and -26.6 cm^{-1} relative to the 0_0^0 of ngpb) probably corresponds to the AB configuration of ngpb$(C_3H_8)_2$ since the binding of the propane molecule above (A position) the ring has little contribution to the overall cluster shift. The BB configuration of ngpb$(C_3H_8)_2$ should have a somewhat larger cluster shift than that found for ntpb$(C_3H_8)_2$ as suggested by the calculations. We therefore assign the bands at -81 cm^{-1} (-32 cm^{-1} relative to the ngpb 0_0^0) and -28.8 cm^{-1} as the 0_0^0 transitions of the BB configuration of ngpb$(C_3H_8)_2$ and ntpb$(C_3H_8)_2$, respectively. Tentative vibronic assignments are found in Table IV.

Figure 6 (top trace) shows the npb$(C_3H_8)_3$ two-color MS spectrum. No attempt is made to assign these data at this time. The relative positions of the major features are given in Table IV.

C. Cluster binding energies

The binding energies of npb-alkane clusters are found through two experiments: two-color MS from high vibronic levels and potential calculations. The binding energies obtained by these two methods are consistent with one another and are similar to those of the comparable toluene–alkane clusters.[2] Two-color MS ion signals are observed for all npb–alkane clusters at the $6b^1$ level (0° + 530 cm^{-1}). Due to the weak intensity of the 1_0^1 transition (10% of the 0_0^0 intensity), no conclusive deter-

TABLE III. Two-color MS absorption features of npb$(C_2H_6)_x$, $x \leq 3$ near the electronic origin.[a]

Energy (vac cm^{-1})	Energy relative to cluster 0_0^0 (cm^{-1})	Energy relative to ntpb 0_0^0 (cm^{-1})	Tentative assignment[b]
npb$(C_2H_6)_1$			
37 502.5	0	−80.6	ngpb(C_2H_6) 0_0^0 B (-31.4 cm^{-1} relative to ngpb 0_0^0)
37 524.9	22.4	−58.3	V_0^1
37 520.3	0	−62.8	ntpb(C_2H_6) 0_0^0 A
37 531.6	11.3	−51.6	X_0^1
37 540.3	20.0	−42.8	Y_0^1
37 550.3	30.0	−32.9	V_0^1
37 556.8	0	−26.3	ntpb(C_2H_6) 0_0^0 B
37 565.1	8.3	−18	X_0^1
37 571.2	14.4	−11.9	Y_0^1
37 579.9	23.1	−3.2	V_0^1
37 596.3	39.5	13.2	V_0^2
npb$(C_2H_6)_2$			
37 486.4	0	−96.7	ngpb$(C_2H_6)_2$ 0_0^0 BB (-47.6 cm^{-1} relative to ngpb 0_0^0)
37 494.6	8.2	−88.5	X_0^1
37 506.2	19.8	−76.9	V_0^1
37 498	0	−85.2	ntpb$(C_2H_6)_2$ 0_0^0 AB
37 519.1	21.1	−64	V_0^1
37 524.7	0	−58.4	ntpb$(C_2H_6)_2$ 0_0^0 AA
37 555.5	30.8	−27.6	V_0^1
37 580.6	55.9	−2.5	V_0^2
37 534.4	0	−48.7	ntpb$(C_2H_6)_2$ 0_0^0 BB
37 544	9.6	−39.1	X_0^1
37 551.1	16.7	−32	Y_0^1
37 555.5	21.	−27.6	V_0^1
37 570.8	36.4	−12.3	V_0^2
npb$(C_2H_6)_3$			
37 490.6		−92.6	
37 500.5		−82.6	
37 512.6		−70.6	
37 519.8		−63.3	
37 528.7		−54.4	
37 535.6		−47.5	
37 548.1		−35	
37 555.5		−27.6	
37 562.1		−21.1	
37 570.7		−12.5	
37 577.1		−6.1	
37 585.5		2.4	

[a] See footnote a for Table II.
[b] See footnote b for Table II.

mination of the ion signal can be made. At 12^1 (0° + 932 cm^{-1}) and 18_a^1 (0° + 966 cm^{-1}) no ion signals for npb$(CH_4)_x$ can be observed. On the other hand, at $18a^1$ a weak, broad signal is found for npb$(C_2H_6)_1$ and a relatively sharp series of features is found for npb$(C_3H_8)_1$. We therefore conclude that the binding energies (D_0) for npb$(CH_4)_1$, npb$(C_2H_6)_1$, and npb$(C_3H_8)_1$ are $530 \leq D_0 \leq 933$ cm^{-1}, $D_0 \sim 930$ cm^{-1}, and $D_0 > 966$ cm^{-1}, respectively, in the first excited singlet state.

The calculated binding energies for the observed clusters are found to fall within the limits of the experimental binding energies cited above. In general, different geometries of the same cluster have very similar binding energies. For example, all npb$(CH_4)_1$ clusters have a calculated binding energy of 700 ± 10% cm^{-1}, all npb$(C_2H_6)_1$ clusters have a binding energy of 900 cm^{-1} ± 5%, and all npb$(C_3H_6)_1$ clusters have a binding energy of 1125 cm^{-1} ± 5%. The npb(solvent)$_2$ clusters vary in a similar manner with binding energies roughly twice those of the respective monosolvated npb. Energy spreads of roughly 10%–15% within a given species are found for the npb(solvent)$_2$ clusters. Given the calculational uncertainties for a particular set of potential parameters and a particular potential form (exp-6), we consider the binding

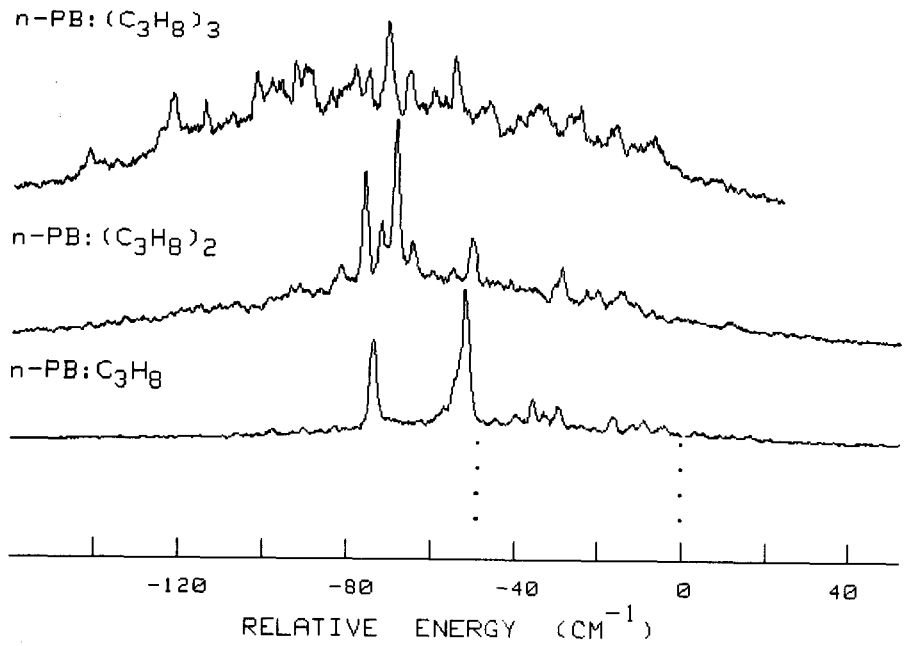

FIG. 6. Two-color MS spectra of the npb$(C_3H_8)_x$, $x \leq 3$ observed at the 0_0^0 with 2% C_3H_8 in the expansion with helium carrier gas. Intensity scale is different for each cluster. Experimental conditions: see Fig. 1.

energy differences for a given cluster series (i.e., ntpb$(CH_4)_2$, ngpb$(CH_4)_2$, AB, AA, BB) to be of no fundamental significance.

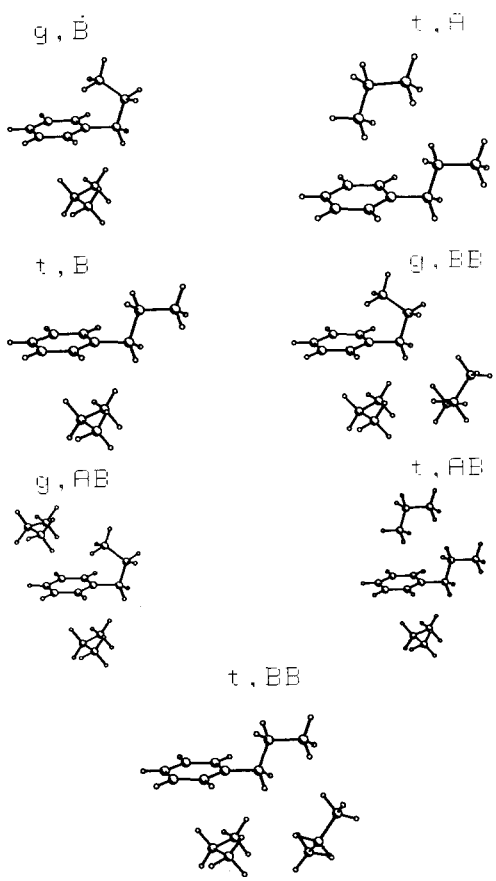

FIG. 7. Minimum energy configurations of npb$(C_3H_8)_x$, $x \leq 2$ obtained from potential calculations. The order of the configurations is arranged according to Table IV. Detailed atomic coordinates of the clusters can be provided upon request.

IV. DISCUSSION

Both calculations and experiments find that more than one nearly isoenergetic conformer exists for many of the clusters. Analysis of the spectra would have been extremely difficult and much less informative without the aid of the calculations. Potential calculations offer a viable alternative to high resolution rotational spectroscopy of clusters (presently under way in our laboratory, nonetheless). The admittedly crude exp-6 potential model employed in these calculations faithfully predicts the binding energies of toluene–alkane,[2a] benzene–alkane,[2b] and npb–alkane clusters. Replacing the composite atom–atom potential parameters with *ab initio* calculations of the intermolecular interactions between the alkane and npb molecules would be an improvement, however. Addition of charge terms and/or multipole molecular moments would also probably make cluster geometries more accurate and reliable.

In the discussion below a more in depth treatment of cluster geometry, cluster shift and the possible relative motions of the propyl chain in the npb molecule will be presented.

A. Cluster geometry

Cluster geometries are mainly derived from potential calculations and expectations based on experience with benzene and toluene systems.[2] In general two configurations, above (A) and below (B) the plane of the aromatic ring as defined by the propyl chain (A), with roughly equal binding energies, are predicted for ngpb$(C_yH_{2y+2})_1$ and ntpb$(C_yH_{2y+2})_1$ ($y \leq 3$). These geometries are depicted in Figs. 3, 5, and 7. In the A configurations of ntpb$(C_yH_{2y+2})_1$ the alkane molecules are nearly centered above the aromatic ring and apparently interact significantly with the π system of the ring. The alkane molecules

TABLE IV. Two-color MS absorption features of npb$(C_3H_8)_x$, $x \leq 3$ near the electronic origin.[a]

Energy (vac cm^{-1})	Energy relative to cluster 0_0^0 (cm^{-1})	Energy relative to ntpb 0_0^0 (cm^{-1})	Tentative assignment[b]
npb$(C_3H_8)_1$			
37 509.1	0	−74.1	ngpb$(C_3H_8)_1$ 0_0^0 B (-24.9 cm^{-1} relative to ngpb 0_0^0)
37 528.1	19	−55	V_0^1
37 543	34.9	−40.1	V_0^2
37 530.9	0	−52.2	ntpb$(CH_3H_8)_1$ 0_0^0 A
37 547.1	16.2	−36.1	X_0^1
37 550.1	19.2	−33	Y_0^1
37 553.3	22.4	−29.8	V_0^1
37 570.8	39.9	−12.3	V_0^2
37 566.3	0	−16.9	ntpb$(C_3H_8)_1$ 0_0^0 B
37 573.7	7.4	−9.4	X_0^1
37 578.4	12.1	−4.7	Y_0^1
37 586.5	20.2	3.4	V_0^1
npb$(C_3H_8)_2$			
37 502	0	−81.1	ngpb$(C_3H_8)_2$ 0_0^0 BB (-32 cm^{-1} relative to ngpb 0_0^0)
37 511.2	9.2	−71.9	X_0^1
37 523.7	21.7	−59.5	V_0^1
37 507.4	0	−75.8	ngpb$(C_3H_8)_2$ 0_0^0 AB (-26.6 cm^{-1} relative to ngpb 0_0^0)
37 518.6	11.2	−64.5	X_0^1
37 528.6	21.2	−54.6	V_0^1
37 514.6	0	−68.5	ntpb$(C_3H_8)_2$ 0_0^0 AB
37 532.9	18.3	−50.2	V_0^1
37 554.3	0	−28.8	ntpb$(C_3H_8)_2$ 0_0^0 BB
37 561.4	7.1	−21.7	X_0^1
37 568.5	14.1	−14.7	V_0^1
npb$(C_3H_8)_3$			
37 441.8		−141.4	
37 461.2		−121.9	
37 468.9		−114.2	
37 481		−102.1	
37 492		−91	
37 512		−71	
37 517.1		−66	
37 528.1		−55	
37 535.6		−47.5	
37 547.7		−35.4	
37 556.5		−26.6	
37 565.9		−17.2	
37 574.9		−8.2	

[a] See footnote a for Table II.
[b] See footnote b for Table II.

in the ngpb$(C_yH_{2y+2})_1$ clusters are, however, displaced 1.25 Å along the X axis (C_1–C_7) away from the ring center and considerable interaction is found between the terminal methyl group of the propyl chain and the alkane molecule in this configuration (see Figs. 3, 5 and 7). Thus the geometry in such complexes leads to an apparently small effective interaction between the solvent molecules and the π cloud of the aromatic ring. Both the two B configurations of npb$(C_yH_{2y+2})_1$ are quite similar in terms of coordinates, with the alkane solvent molecules displaced along the $+X$ direction toward the propyl chain: the $+X$ direction displacement of the solvent is about 10% greater for ntpb$(CH_4)_1$ than for ngpb$(CH_4)_1$. Three general configurations of substantial binding energy are calculated for npb$(C_yH_{2y+2})_2$ clusters: AB, AA, and BB. The AB configuration geometry is essentially the composite geometry of the configuration A and B of npb$(C_yH_{2y+2})_1$ clusters. Solvent molecules do not interact strongly with each other if they are on opposite sides of the aromatic ring. The AA configuration of ntpb$(CH_4)_2$ (Fig. 3) features

one methane molecule centered above the ring and one over the propyl chain. However, the AA configuration of ntpb$(C_2H_6)_2$ has one ethane over the ring and the other displaced considerably in the $-X$ direction presumably due to ethane–ethane interactions (Fig. 5). The BB configurations of npb$(C_yH_{2y+2})_2$ are in general quite similar (Figs. 3, 5, and 7) to each other.

The ngpb(solvent)$_1$ A configurations are missing in the spectral assignments for all three alkane solvents. It is of course possible that these features are hidden under others. However, since the cluster binding energies for the A, B, *g*, *t* clusters for a given solvent are so similar, the intensity differences are difficult to explain on the basis of energy considerations. At present we believe the A configurations of the ngpb(solvent)$_1$ clusters are only present in the beam in small concentrations. In Ref. 2 we describe the cluster nucleation process in the beam as occurring through the interaction of solute monomers and solvent dimers or higher clusters. We suggest in this situation that the *g*A configurations are not kinetically favorable. The AB ngpb(solvent)$_2$ species may then arise from the *g*B configuration of ngpb(solvent)$_1$, which perhaps in some manner alters the formation rate of *g*A binding.

These observations suggest that the two conformations of the propyl chain in npb have a significant influence on cluster geometry and the effective interactions between the solvent alkane molecules and the aromatic ring. Note, however, that the above conclusion is derived from a calculation in which the propyl chain is held fixed. Nonetheless, the overall cluster geometry should not vary essentially if the propyl chain were released because the experimental data suggest that significant rotational (nonlibrational) motion of the propyl chain can only occur about the C_8–C_9 band (see below).

B. Cluster shift

The binding of two uncharged molecules is typically associated with molecular polarizabilities or dispersion forces.[9] Changes in these interactions upon electronic excitation of one of the molecules gives rise to the cluster red shift. Therefore, the measured cluster shift depends upon the solvent polarizability and changes in the local solute binding site polarizability upon excitation of the solute.

Since there is no direct information on the polarizability of npb in the literature, we assume that it is similar to, but larger than, that of toluene (11.86 Å^3)[10]: this larger polarizability would probably result in a larger polarizability change upon electronic excitation. A larger cluster shift is thereby to be expected for a ring centered ntpb$(CH_4)_1$ cluster than for a ring centered toluene $(CH_4)_1$ cluster. In fact, the observed shifts for ntpb$(CH_4)_1$ (A configuration) and toluene $(CH_4)_1$ are -51 and -44 cm^{-1}, respectively.

In Sec. III a number of origin assignments are made which depend on comparisons between configurations for cluster spectral shifts and published results for simpler systems.[2] Below we present some detailed discussion which should help to clarify further some of the choices. The solvent/solute interactions are quite different for the A and B configurations of ntpb$(C_yH_{2y+2})_1$ (see Figs. 3, 5, and 7). Potential calculations demonstrate that the effective interaction between the solvent molecule and aromatic π cloud is significantly larger for the A than the B configuration of ntpb. In addition, the calculations yield similar atomic coordinates for the B configurations of both nbpb$(C_yH_{2y+2})_1$ and ntpb$(C_yH_{2y+2})_1$ with $y = 2, 3$. We have thus assigned, in accordance with previous results,[2] the larger cluster shifts to the A configurations of ntpb$(C_yH_{2y+2})_1$. If the assignments are changed to give smaller spectral shifts to the A configurations and larger ones to the B configurations, comparable large shifts ($\sim$60 cm^{-1}) would be expected for ngpb$(C_yH_{2y+2})_1$ complexes: such shifts are clearly not observed in the spectra. This observation and analysis serve as independent confirmation of the relationship between cluster spectral shift and solute/π-cloud interaction: solvent molecules create large shifts if they are closely coordinated to the aromatic π system of the solute.

The cluster shifts for the B configurations of ngpb$(CH_4)_1$ and ntpb$(CH_4)_1$ are -44 and -26 cm^{-1}, respectively. This trend in shifts is primarily associated with the increased interaction of the solvent with the π system of the aromatic ring and can be in general followed through the series of systems discussed in this work. Nonetheless, other factors can contribute to the size of the cluster shift. In particular, local solute binding site polarizability can play a role in the overall spectral shift: for example, the $-Z$ component of the molecular polarizability of ngpb is probably larger than the $-Z$ polarizability of ntpb. This consideration would suggest a larger cluster shift for the B configuration of ngpb$(C_yH_{2y+2})_1$ than for the comparable ntpb$(C_2H_{2y+2})_1$ complex even if the effective interaction between the solvent molecule and the π cloud of the solute were essentially the same. This trend is indeed observed throughout the npb$(C_yH_{2y+2})_1$ series.

Further subtle variations in the npb$(C_yH_{2y+2})_{2,3}$ cluster spectral shift can be found for the case in which two solvent molecules are on the same side of the solute aromatic ring (BB or AA, etc.). In this geometry the two solvent molecules can interact with one another and thereby alter the cluster spectral shift. This effect is most pronounced for solvents of large polarizability such as propane. In fact, a smaller cluster shift is found for the BB configuration of npb$(C_3H_8)_2$ than for npb$(C_2H_6)_2$ or npb$(CH_4)_2$.

The cluster shifts of npb$(C_yH_{2y+2})_3$ cannot be readily determined based on the present data. The intense background (see Figs. 2, 4, and 6) may suggest a number of conformers present in the beam, each contributing to the overall congested intensity pattern.

C. Propyl chain motion

As mentioned in Sec. III, two weak features at 37 572.9 cm^{-1} (+38.9 cm^{-1} relative to the ngpb 0_0^0) and 37 613.9 cm^{-1} (+30.7 cm^{-1} relative to the ntpb 0_0^0) are observed in the two-color MS spectrum of npb (see Fig.

1). These two weak features are most likely not due to hot bands because their relative intensities remain virtually unchanged over a wide range of expansion conditions. We assume then that the two features arise from transitions involving a change in the propyl chain motion. Toluene evidences two such features at 53.5 and 76.5 cm^{-1} due to methyl motion.[2] The comparison of ngpb, ntpb, and toluene librational frequencies leads one to associate the corresponding motions to CH_3 hindered rotations.

The correlation times for rotations of end groups about bonds 1, 2, 3 in alkanes are all in the picosecond regime.[11,12] If relatively free rotation occurs about the phenyl–alkyl (C_1–C_7, X axis) or the ethane (C_7–C_8) bonds, differences between t, g, and A, B configurations resulting in sharp spectral features are difficult to understand. In addition, recall that a ring centered ngpb$(He)_1$ complex is formed but not a ngpb$(He)_2$ complex[3(a),5] and that the various configurations of npb$(CH_4)_1$ have large and different cluster red shifts. These energy differences, line shapes, and apparent stability of the various cluster configurations further suggest that the two weak features at 37 572.9 and 37 613.9 cm^{-1} are most likely due to the CH_3 rotational or librational motion about the C_8–C_9 bond. The predicted cluster geometries would thereby remain unaffected by the motion.

V. CONCLUSIONS

The important information that emerges from this study can be summarized as follows:

(1) Atom–atom potential calculations provide a viable method for predicting cluster geometry and binding energy for the npb–alkane system. The calculated binding energies for npb$(CH_4)_1$, npb$(C_2H_6)_1$, and npb$(C_3H_8)_1$ are 770, 960, and 1170 cm^{-1}, respectively. These values are consistent with those obtained by two-color MS detection methods.

(2) The cluster shift is a complex function of solvent polarizability, changes in local binding site polarizability of the solute upon excitation, and solvent/solute and solvent/solvent interactions. In general, however, the cluster shift scales with the effective interaction between the solvent molecules and the π cloud of the aromatic ring of npb. Similar behavior is observed in the comparable toluene–alkane and benzene–alkane systems.

(3) Solvation of npb by simple alkanes has little apparent effect on the geometry of the npb monomer.

(4) Motion of the alkane chain is assumed to occur about the C_8–C_9 bond so that only the terminal CH_3 group can rotate within the lifetime of the excited state (80 ns).

[1] (a) E. R. Bernstein, K. S. Law, and M. Schauer, J. Chem. Phys. **80,** 634 (1984); (b) A. Amirav, U. Even, and J. Jortner, *ibid.* **75,** 2489 (1981).
[2] (a) E. R. Bernstein, K. S. Law, and M. Schauer, J. Chem. Phys. **82,** 726 (1985); (b) E. R. Bernstein and M. Schauer, *ibid.* **82,** 736 (1985).
[3] (a) J. B. Hopkins, D. E. Powers, and R. E. Smalley, J. Chem. Phys. **72,** 5039 (1980); (b) **72,** 5049 (1980).
[4] K. Watanabe, T. Nakayama, and J. Mottl, J. Quant. Spectrosc. Radiat. Transfer **2,** 369 (1962).
[5] K. S. Law and E. R. Bernstein (unpublished results).
[6] D. E. Williams, Acta. Crystallogr. Sect. A **36,** 715 (1980).
[7] H. Yasuda, J. Chem. Phys. **73,** 3722 (1980).
[8] K. S. Law and E. R. Bernstein (unpublished results).
[9] M. J. Ondrechen, Z. Berkovitch-Yellin, and J. Jortner, J. Am. Chem. Soc. **103,** 6586 (1981).
[10] R. Kaila, L. Dixit, and P. L. Gupta, Acta. Phys. Acad. Sci. Hung. **42,** 237 (1977).
[11] J. A. Nairn and C. L. Braun, Chem. Phys. Lett. **52,** 385 (1977).
[12] J. Prochorow, W. Hopewell, and M. A. El-Sayed, Chem. Phys. Lett. **65,** 410 (1979).